Study of hydrogen absorption by $ZrMnFe_{1-x}Co_x$ (x = 0.2, 0.4, 0.5 and 0.6) alloys

2002 J. Phys.: Condens. Matter 14 3939

(http://iopscience.iop.org/0953-8984/14/15/308)

INSTITUTE OF PHYSICS PUBLISHING JOURNAL OF PHYSICS: CONDENSED MATTER

J. Phys.: Condens. Matter **14** (2002) 3939–3949 PII: S0953-8984(02)29097-9

Study of hydrogen absorption by $ZrMnFe_{1-x}Co_x$ (x = 0.2, 0.4, 0.5 and 0.6) alloys

N Mani, T R Kesavan and S Ramaprabhu[1]

Alternative Energy Technology and Magnetism and Magnetic Materials Laboratory, Indian Institute of Technology Madras, Chennai 600 036, India

E-mail: ramp@mmm.iitm.ernet.in

Received 25 September 2001, in final form 14 February 2002
Published 4 April 2002
Online at stacks.iop.org/JPhysCM/14/3939

Abstract

Hydrogen absorption isotherms have been obtained for the C14-type hexagonal-structured alloys $ZrMnFe_{1-x}Co_x$ ($x = 0.2, 0.4, 0.5$ and 0.6) in the temperature and pressure ranges $30 \leqslant T/^{\circ}C \leqslant 100$ and $0.1 \leqslant P/\text{bar} \leqslant 40$ using a high-pressure unit based on the pressure reduction method. The powder x-ray diffractograms show that the lattice constants and the unit-cell volume for $ZrMnFe_{1-x}Co_x$ ($x = 0.2$, 0.4, 0.5 and 0.6) alloys decrease with increase of x_{Co}. The hydrogen absorption isotherms show the presence of a single plateau region ($\alpha+\beta$) in the temperature and pressure ranges studied and it is found that the plateau pressure and plateau slope at any given temperature increase with increase of the x_{Co}-content, except in the case of $ZrMnFe_{0.5}Co_{0.5}$ wherein the hydrogen absorption plateau slope is found to be smaller due to the ordering of the alloy. The dependence of the thermodynamics of the dissolved hydrogen in $ZrMnFe_{1-x}Co_x$–H ($x = 0.2$, 0.4, 0.5 and 0.6) systems in the temperature range 30–50 °C on the hydrogen concentration shows the different phase regions (α, $\alpha+\beta$, β) seen in the hydrogen absorption isotherms. The powder x-ray diffractograms of the hydrides of $ZrMnFe_{0.8}Co_{0.2}$ show that the formation of different phases is manifested in the isotherms without there being any structural change and the inclusion of hydrogen in the interstitial sites expands the unit-cell volume by about 21%. Comparison of the hydrogen absorption kinetics of $ZrMnFe_{1-x}Co_x$ with that of the corresponding Ni alloys in similar experimental conditions shows that the kinetics is slow in the $ZrMnFe_{1-x}Co_x$ alloys.

1. Introduction

Zirconium-based C14 Laves-phase AB_2 alloys have been the focus of attention recently due to their potential as hydrogen storage materials and electrode materials for Ni–MH batteries [1,2].

[1] Author to whom any correspondence should be addressed.

They have remarkable hydrogen storage characteristics and their hydrogen storage properties can be significantly modified by an alloying procedure in which Zr is partially replaced by other suitably chosen elements. $ZrMn_2$ has excellent hydrogen storage capacity but the desorbing properties are quite poor and the hydrogen desorbing capacity can be increased by the partial replacement of Mn by other chosen elements. Recently, the hydrogen storage properties in Zr-based Laves-phase C14 alloys have been studied in order to find their suitability for use in Ni–MH batteries [3, 4].

From the study of the hydrogen storage properties of Co-substituted C15 Laves-phase $Zr_xHo_{1-x}Fe_2$ ($x = 0.1$, 0.2 and 0.3) and rhombohedral $Zr_xTb_{1-x}Fe_3$ ($x = 0.1$, 0.2 and 0.3) alloys, it has been observed in our laboratory that the substitution of Co at Fe sites in these alloys in the mole ratio 1:1 remarkably reduces the plateau slope due to the increase in the degree of order [5, 6]. Our recent investigations of the hydrogen storage properties of $ZrMnFe_{1-x}Ni_x$ ($x = 0.2$, 0.4, 0.5 and 0.6) alloys [7] also revealed that the partial replacement of Ni results in increases of the plateau pressure and the plateau slope except for $ZrMnFe_{0.5}Ni_{0.5}$, for which the plateau slope is less—which can be attributed to the increase in the degree of order of the alloy due to the presence of Fe and Ni in the mole ratio 1:1. In view of these findings, in the present work we aimed to study the hydrogen storage properties of Zr-based C14 Laves-phase $ZrMnFe_{1-x}Co_x$ ($x = 0.2$, 0.4, 0.5 and 0.6) alloys in the ranges $0.1 \leqslant P/\text{bar} \leqslant 40$ and $30 \leqslant T/^\circ\text{C} \leqslant 100$ using a high-pressure apparatus based on Sievert's method in order to find the influence of Co on the hydrogen storage properties and especially on the plateau slope when Co and Fe are in the 1:1 mole ratio.

2. Experimental details

2.1. Sample preparation and powder x-ray diffractograms

$ZrMnFe_{1-x}Co_x$ ($x = 0.2$, 0.4, 0.5 and 0.6) alloys were prepared in an arc furnace under an argon atmosphere. They were melted in stoichiometric proportions. 6 wt% of excess Mn was added to the total mixture following the normal procedure, since the vapour pressure of Mn is very high. The alloy buttons were remelted several times by turning them over to ensure homogeneity. The weight loss of the sample during their preparation was <0.7%. Since as-formed alloys show single-phase formation, no annealing treatment was given. The x-ray powder diffraction patterns were taken with Fe Kα radiation, with Si as the standard.

2.2. Hydrogen absorption isotherms and kinetics studies

Hydrogen absorption pressure–composition–temperature (PCT) relationship and kinetics data were collected by a conventional gasometric technique. An apparatus based on the pressure reduction method and operating in the temperature range 30–300 °C and in the pressure range 0.1–100 bar was employed [8]. Prior to the measurements, the hydrogen absorption system was flushed with hydrogen several times and evacuated each time to 10^{-6} Torr. The alloys were first activated for hydrogen absorption by degassing in high vacuum (10^{-6} Torr) at 100 °C for about 2 h, then allowed to interact with hydrogen at 20 bar and then slowly cooled to room temperature. This procedure was repeated several times in order to produce fresh surfaces for quantitative and rapid measurements. After this activation procedure, the alloys were degassed at 200 °C under a vacuum of 10^{-6} Torr for 2 h before each cycle of hydrogen absorption. The pressure–composition isotherms were obtained by calculating the hydrogen concentration in the sample ($r = n_H/n_{f.u.}$) from the pressure drop during the absorption reaction at constant volume and constant temperature. Following each run, the sample was degassed and a new

Table 1. The values of a and 'c, with accuracies of 0.002 and 0.003 Å respectively. The values within the brackets are for the corresponding Ni alloys, with accuracies of 0.003 and 0.006 Å respectively.

Alloy	a (Å)	c (Å)	v (Å^3)	$-(\Delta V/V)$ (%)	ANOE
ZrMnFe	5.011	8.202	178.4	—	6.33
$ZrMnFe_{0.8}Co_{0.2}$	5.007	8.195	177.9	0.28	6.40
	(5.008)	(8.196)	(178.0)	(0.22)	
$ZrMnFe_{0.6}Co_{0.4}$	5.003	8.192	177.6	0.45	6.47
	(5.008)	(8.182)	(177.7)	(0.39)	
$ZrMnFe_{0.5}Co_{0.5}$	4.999	8.179	177.0	0.78	6.50
	(5.004)	(8.174)	(177.3)	(0.62)	
$ZrMnFe_{0.4}Co_{0.6}$	4.995	8.170	176.5	1.07	6.53
	(4.998)	(8.167)	(176.7)	(0.95)	
Alloy	a (Å)	c (Å)	v (Å^3)	$(\Delta V/V)$ (%)	
$ZrMnFe_{0.8}Co_{0.2}$	5.007	8.195	177.9	—	
$ZrMnFe_{0.8}Co_{0.2}H_{2.1}$ (α)	4.995	8.172	176.6	—	
(β)	5.314	8.668	212.0	19.17	
$ZrMnFe_{0.8}C0_{0.2}H_{2.7}$ (β)	5.348	8.719	216.0	21.42	

run started with an initial pressure different from the foregoing one. The kinetics data were collected by recording the change in pressure as a function of time at constant temperature.

3. Results and discussion

3.1. Crystal structure

The $ZrMnFe_{1-x}Co_x$ ($x = 0.2, 0.4, 0.5$ and 0.6) alloys crystallize in the C14 hexagonal structure (space group $P6_3/mmc$) as confirmed by the powder x-ray diffraction studies taken with Fe Kα radiation at room temperature (figure 1). The average number of outer electrons (ANOE) in these alloys is less than 7 indicating the preference for the formation of C14 structure (table 1). Since the changes in the unit-cell parameters are very small, the lattice parameters have been precisely obtained using Si as the standard by mixing Si with the alloys while taking the diffractograms. In the hexagonal representation, the lattice parameters, a, c and the unit-cell volume (v), were evaluated using a least-squares refinement technique (table 1). The lattice constants and the unit-cell volume of $ZrMnFe_{1-x}Co_x$ decrease with increase of Co content due to Co having a smaller atomic radius than Fe. The variations of a, c and v for $ZrMnFe_{1-x}Co_x$ alloys can be given as a (Å) $= 5.01 - 0.026x_{Co}$, c (Å) $= 8.21 - 0.05x_{Co}$ and v (Å^3) $= 179 - 2.98x_{Co}$. For a particular value x, the decrease in the unit-cell volume is more in $ZrMnFe_{1-x}Co_x$ than in $ZrMnFe_{1-x}Ni_x$ [7].

3.2. P–C isotherm

The P–C isotherms measured for the system $ZrMnFe_{1-x}Co_x$ ($x = 0.2$, 0.4, 0.5 and 0.6) in the temperature and pressure ranges $30 \leqslant T/^\circ C \leqslant 100$ and $0.1 \leqslant P/\text{bar} \leqslant 30$ are shown in figures 2–5 respectively. These isotherms indicate that there are two single-phase (α and β) regions and one mixed-phase ($\alpha + \beta$) region in the temperature and pressure ranges studied. The maximum hydrogen concentration is found to be around 3.3 hydrogen atoms per

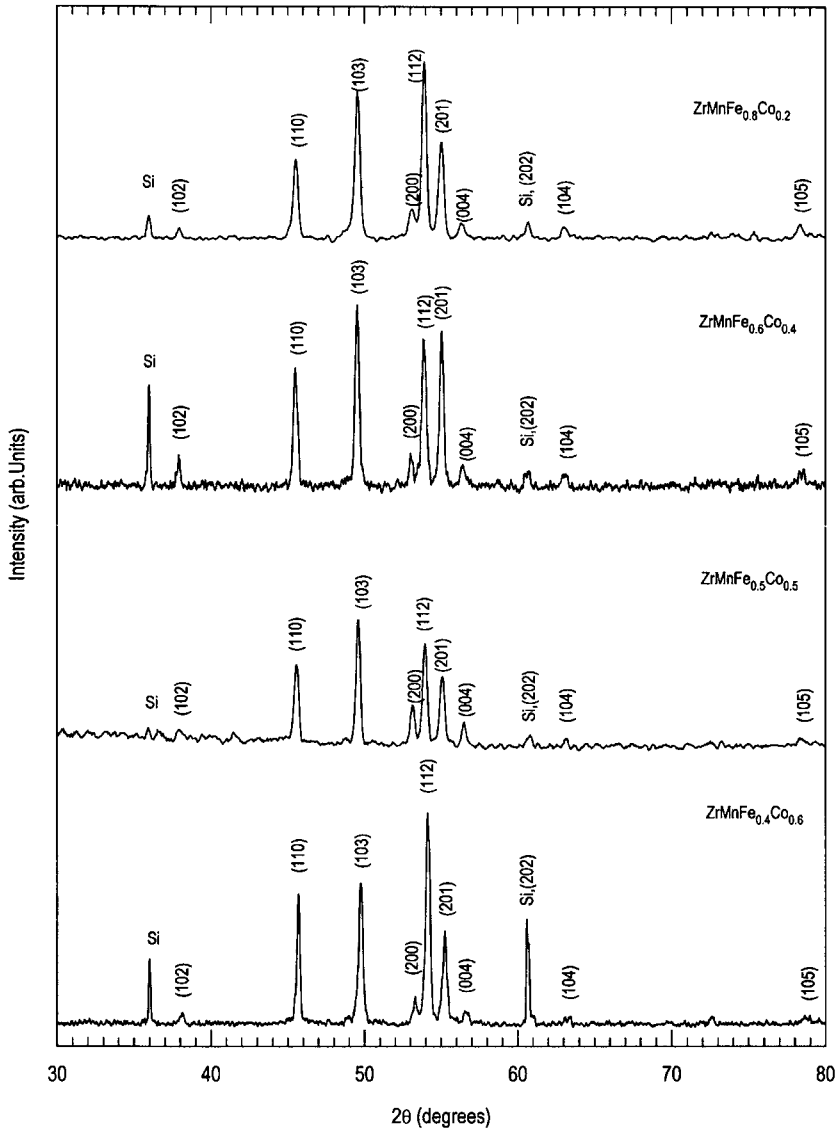

Figure 1. Powder x-ray diffractograms of the alloys $ZrMnFe_{1-x}Co_x$–H ($x = 0.2$, 0.4, 0.5 and 0.6) taken with Fe Kα radiation.

formula unit at 40 bar and 30 °C in $ZrMnFe_{0.5}Co_{0.5}$. At any particular temperature, the plateau pressure $P_{\alpha\rightarrow\beta}$ (at $r = 2$; see figures 2–5) increases with increase in Co content due to the contraction in the unit-cell volume (table 1) as observed in $ZrMnFe_{1-x}Ni_x$ ($x = 0.2$, 0.4, 0.5 and 0.6) alloys. At any fixed x, the increase in $P_{\alpha\rightarrow\beta}$ is greater for the Co system than for Ni system [7] due to the larger contraction of unit-cell volume in $ZrMnFe_{1-x}Co_x$. The plateau slope (plateau slope $= \ln(P_{H/M=2.5}/P_{H/M=0.5})$ at 30 °C) also increases with increase of x_{Co} except for $ZrMnFe_{0.5}Co_{0.5}$, for which the plateau slope is less (see figures 2–5)—which can be attributed to the increase in the degree of order of the alloy due to the presence of Fe and Co in the mole ratio 1:1 as observed in $ZrMnFe_{0.5}Ni_{0.5}$ [7]. Figure 6 gives the exponential

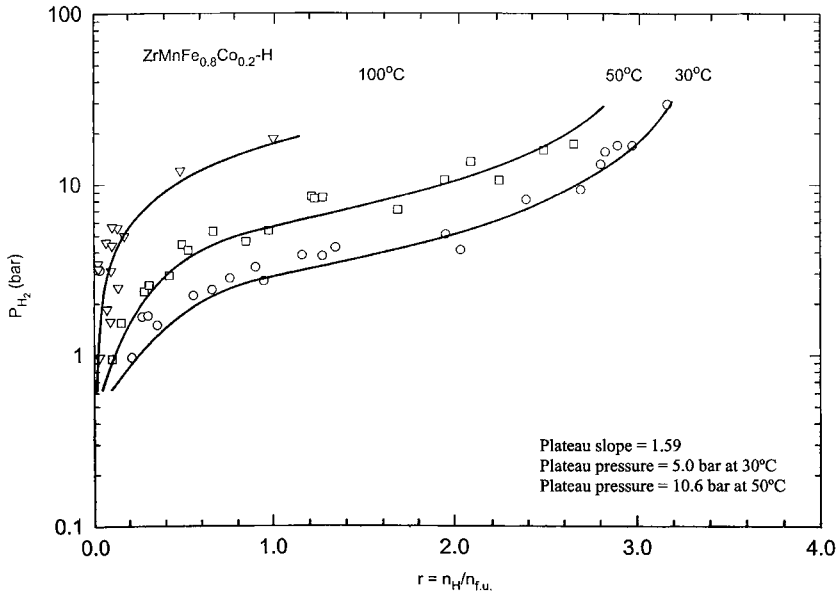

Figure 2. Hydrogen absorption isotherms of $ZrMnFe_{0.8}Co_{0.2}$.

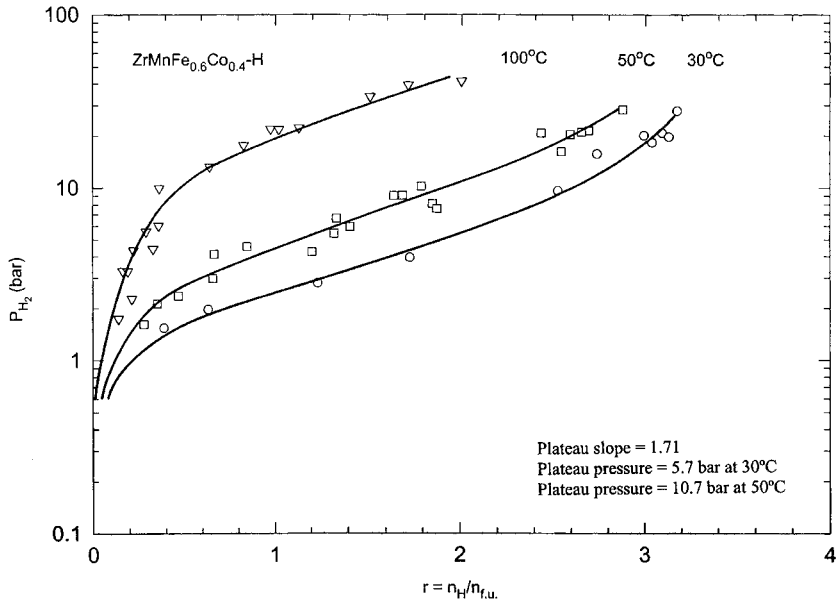

Figure 3. Hydrogen absorption isotherms of $ZrMnFe_{0.6}Co_{0.4}$.

dependence of the plateau pressure at 30 and 50 °C on the unit-cell volume of $ZrMnFe_{1-x}Co_x$. The increase of $P_{\alpha\rightarrow\beta}$ at any particular temperature with decrease in the unit-cell volume is due to the increase in the strain energy necessary to accommodate the hydrogen atoms in the interstitial sites as observed in $LaNi_5$ and its substitutes [9, 10].

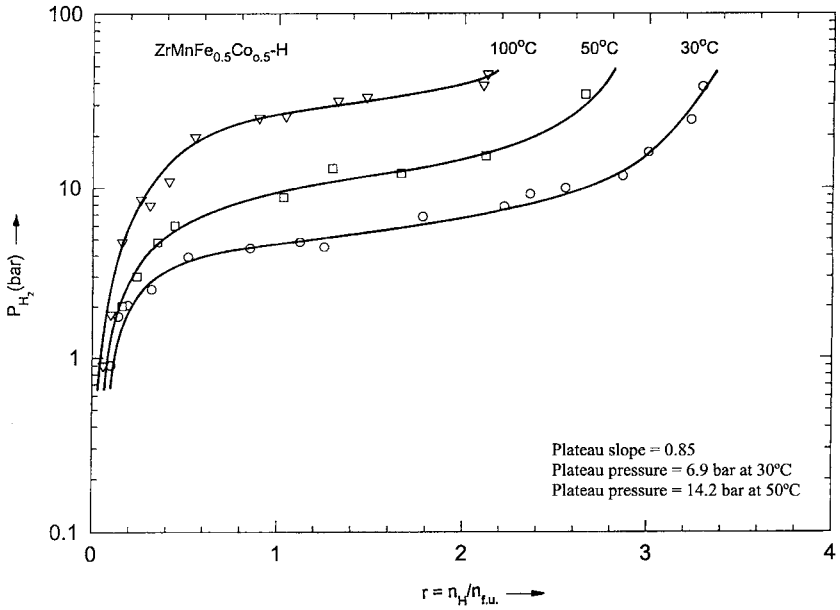

Figure 4. Hydrogen absorption isotherms of $ZrMnFe_{0.5}Co_{0.5}$.

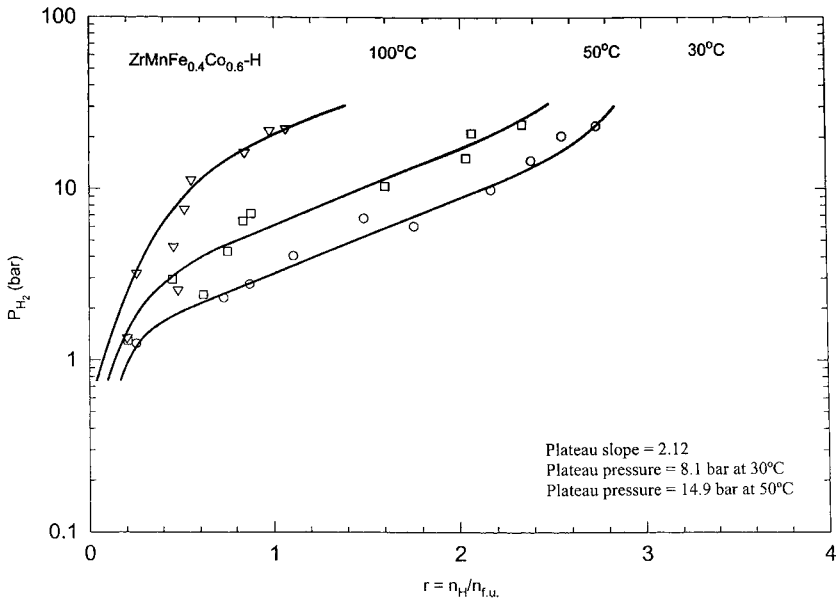

Figure 5. Hydrogen absorption isotherms of $ZrMnFe_{0.4}Co_{0.6}$.

3.3. Thermodynamics of dissolved hydrogen

The relative partial molar enthalpy (ΔH_H) and relative partial molar entropy (ΔS_H) of dissolved hydrogen in $ZrMnFe_{1-x}Co_x$–H can be obtained at any particular concentration of hydrogen

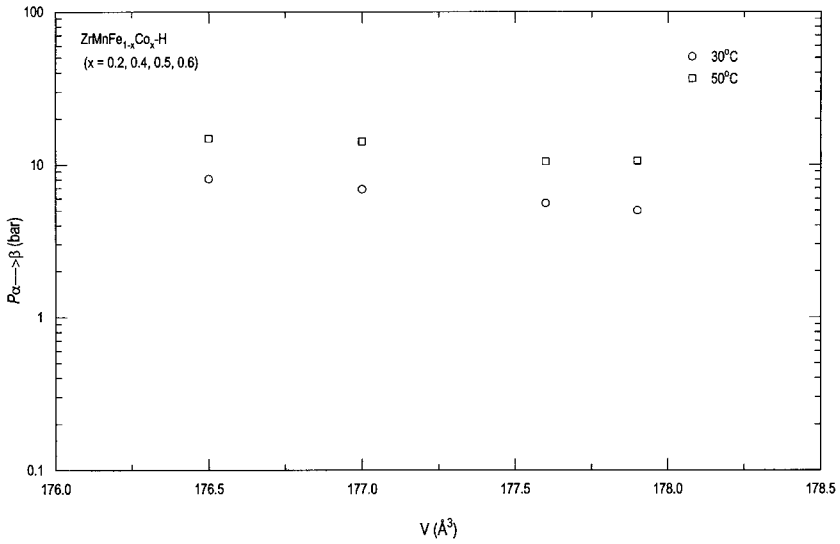

Figure 6. The variation of plateau pressure ($P_{\alpha\rightarrow\beta}$) with unit-cell volume in $ZrMnFe_{1-x}Co_x$–H.

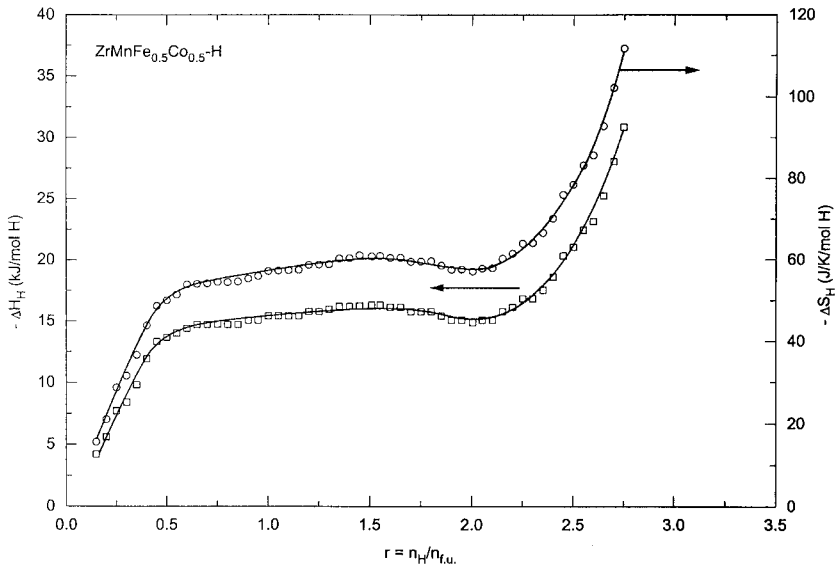

Figure 7. The dependence of ΔH_H and ΔS_H on the hydrogen concentration in $ZrMnFe_{0.5}Co_{0.5}$–H.

from the van't Hoff equation [11]:

$$\ln P_{H_2} = 2\left(\frac{\Delta H_H}{RT} - \frac{\Delta S_H}{R}\right).$$

ΔH_H and ΔS_H for dissolved hydrogen for a particular r-value are obtained by a least-squares technique from the slope and intercept of $\ln P_{H_2}$ and $(1/T)$ plots, respectively. Since in an alloy–hydrogen system, the heat of formation is different for single- and two-phase regions, the variation of ΔH_H as a function of the hydrogen concentration is useful for identification

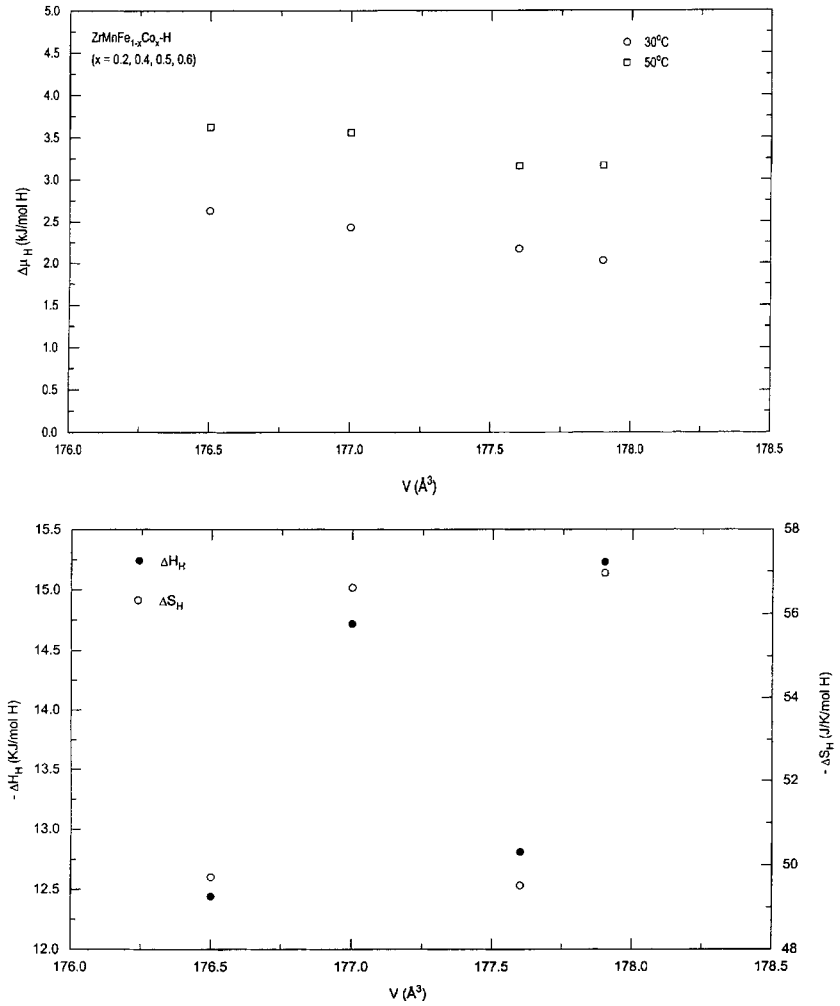

Figure 8. The dependence of $\Delta\mu_{\mathrm{H}}$, $\Delta H_{\mathrm{H}}^{\alpha\rightarrow\beta}$ and $\Delta S_{\mathrm{H}}^{\alpha\rightarrow\beta}$ on the unit-cell volume in $ZrMnFe_{1-x}Co_x$–H systems.

of different phases and the phase boundaries. For example, the dependence of ΔH_{H} and ΔS_{H} on r in $ZrMnFe_{0.5}Co_{.5}$–H is shown in figure 7, which indicates the existence of regions of the phases α, $\alpha+\beta$, β as seen in the isotherms. The dependences of $\Delta H_{\mathrm{H}}^{\alpha\rightarrow\beta}$, $\Delta S_{\mathrm{H}}^{\alpha\rightarrow\beta}$ (calculated for the range 30–50 °C) and the Gibbs free energy $\Delta\mu_{\mathrm{H}}(\Delta\mu_{\mathrm{H}} = \Delta H_{\mathrm{H}} - T\,\Delta S_{\mathrm{H}})$ at 30 and 50 °C) for $ZrMnFe_{1-x}Co_x$–H ($x = 0.2$, 0.4, 0.5 and 0.6) on the unit-cell volume of the alloys are shown in figure 8. The variation of $\Delta\mu_{\mathrm{H}}$ with the unit-cell volume of alloys suggests that the strain energy necessary to accommodate the interstitial hydrogen increases with decrease of size of these interstitial sites by virtue of the decrease in unit-cell volume of $ZrMnFe_{1-x}Co_x$ with increase of the Co content.

3.4. X-ray diffractograms of alloy hydrides

Hydrogenation of AB_5 alloys such as $SmCo_5$ and $PrCo_5$ changes their structure from hexagonal $CaCu_5$ to an orthorhombic structure, whereas AB_3 alloys such as $TbFe_3$, YFe_3 and $ErFe_3$

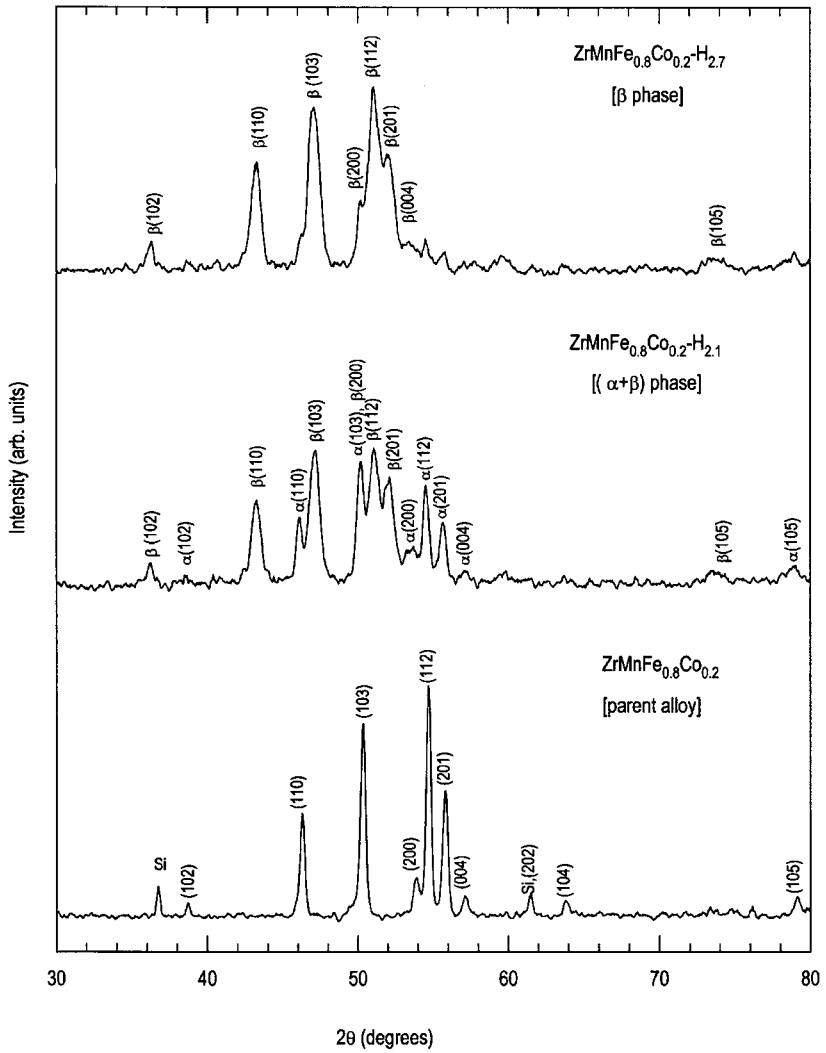

Figure 9. Powder x-ray diffractograms of $ZrMnFe_{0.8}Co_{0.2}$ and $ZrMnFe_{0.8}Co_{0.2}$–H_y ($y = 1.61$ ($\alpha + \beta$) and $y = 2.91$ (β)) obtained with Fe Kα radiation.

and also $Zr_xTb_{1-x}Fe_3$ retain their $PuNi_3$ structure upon hydrogenation [12–15]. The powder x-ray diffractograms of the present alloy hydrides show that there is no structural change upon hydrogenation. Figure 9 shows the powder x-ray diffractograms for $ZrMnFe_{0.8}Co_{0.2}$–H_y ($y = 2.1$ and 2.7). It can be seen that the diffraction pattern for the hydride in the mixed ($\alpha + \beta$) phase shows two sets of Bragg reflections, each one corresponding to the α- and β-phase components of the alloy hydride (table 1). That of the β-phase is identical to that of the parent alloy with increase in the unit-cell volume. Thus there is only volume expansion upon hydrogenation up to about 21.4% without any change in the crystal structure.

3.5. Kinetics of hydrogen absorption

The hydrogen absorption kinetics during activation in $ZrMnFe_{1-x}Ni_x$ ($x = 0.2$, 0.4, 0.5 and 0.6) alloys revealed that the kinetics of absorption increases with increase of Ni content [7].

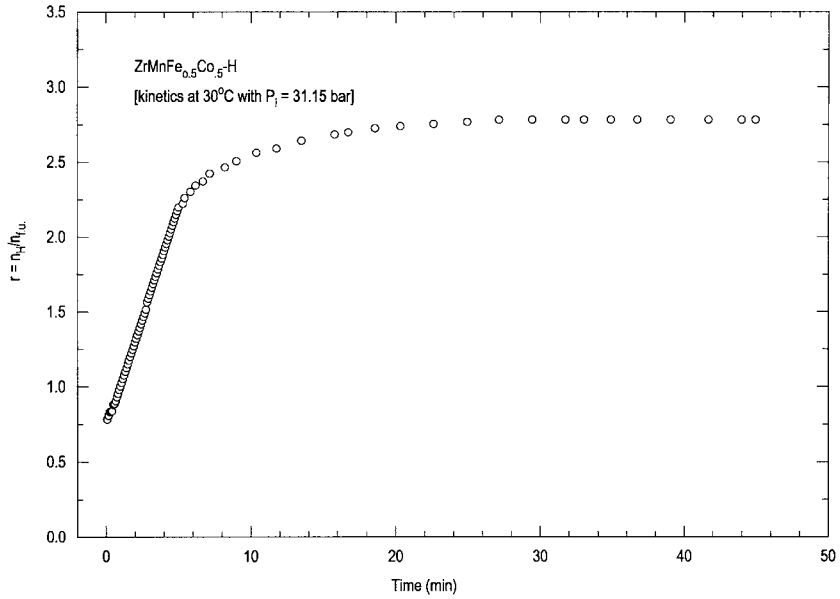

Figure 10. Kinetics of absorption in $ZrMnFe_{0.5}Co_{0.5}$ at 30 °C after several cycles of absorption/desorption.

However, the hydrogen absorption kinetics during activation in the present $ZrMnFe_{1-x}Co_x$ ($x = 0.2$, 0.4, 0.5 and 0.6) alloys at an initial pressure of around 30 bar is quite slow when compared with that of $ZrMnFe_{1-x}Ni_x$ ($x = 0.2$, 0.4, 0.5 and 0.6). Figure 10 shows the kinetics of absorption in $ZrMnFe_{0.5}Co_{0.5}$ at 30 °C after several cycles of absorption/desorption with an initial pressure of 31.15 bar. The hydrogen absorption takes around 30 min even after several cycles of absorption/desorption whereas $ZrMnFe_{0.5}Ni_{0.5}$ requires less than 20 min to attain the equilibrium pressure.

4. Conclusions

Hydrogen absorption isotherms of $ZrMnFe_{1-x}Co_x$–H ($x = 0.2$, 0.4, 0.5 and 0.6) in the ranges $30 \leqslant T/\,^{\circ}\mathrm{C} \leqslant 100$ and $0.1 \leqslant P/\mathrm{bar} \leqslant 40$ reveal that the plateau pressure, at any particular temperature, increases with increase of x_{Co}. In $ZrMnFe_{0.5}Co_{0.5}$, the hydrogen absorption plateau slope is small compared to those of other alloys due to the increase in the degree of order of this alloy caused by the presence of Fe and Co in the mole ratio 1:1. The powder x-ray diffractograms of the alloy hydrides show that there is only volume expansion up to about 21% without any structural transformation. The kinetics of absorption in these alloys is slow compared to that of the corresponding Ni alloys.

Acknowledgments

The authors are grateful to the MNES and CSIR funding agencies for supporting this work. One of the authors (NM) is grateful to IIT Madras for financial support.

References

[1] Chen W-X 2001 *J. Alloys Compounds* **319** 119–23
[2] Wipf H 1997 *Hydrogen in Metals III (Springer Topics in Applied Physics vol 73)* (Berlin: Springer)
[3] Lee S-M, Kim J-H, Lee P and Lee J-Y 2000 *J. Alloys Compounds* **308** 259–68
[4] Nakayama E, Vematsu F, Yamamoto Y and Iwakura C 2001 *Electrochim. Acta* **46** 2693–7
[5] Sivakumar R, Ramaprabhu S, Rama Rao K V S, Mayer B and Schmidt P C 2000 *J. Alloys Compounds* **302** 146–54
[6] Kesavan T R, Ramaprabhu S, Rama Rao K V S and Das T P 1996 *J. Alloys Compounds* **244** 164–9
[7] Mani N, Sivakumar R and Ramaprabhu S 2002 *J. Alloys Compounds* at press
[8] Sivakumar R 2000 Hydrogen solubility studies in certain Zr–Tb–$(Fe, Co)_3$ compounds *PhD Thesis* Indian Institute of Technology, Madras
[9] Percheron-Guegan and Welter J M 1988 Preparation of intermetallics and hydrides *Hydrogen in Intermetallic Compounds—I (Springer Topics in Applied Physics vol 63)* ed L Schlapbach (Berlin: Springer) ch 2A
[10] Takeshita T, Gschneidner K A Jr, Chung Y and McMasters O D 1982 *J. Phys. F: Met. Phys.* **12**
[11] Flanagan T B and Park C N 1988 *Mater. Sci. Forum* **31** 297
[12] Yvon K and Fischer P 1988 *Hydrogen in Intermetallic Compounds—I (Springer Topics in Applied Physics vol 63)* ed L Schlapbach (Berlin: Springer) ch 4, pp 112–13
[13] Malik S K, Pourarian F and Wallace W E 1983 *J. Magn. Magn. Mater.* **40** 27
[14] Buschow K H J 1976 *Solid State Commun.* **19** 421
[15] Sivakumar R, Ramaprabhu S, Rama Rao K V S, Anton H and Schmidt P C 1999 *J. Alloys Compounds* **285** 143–9